Bioorganic & Medicinal Chemistry 19 (2011) 7401–7406

Contents lists available at SciVerse ScienceDirect

Bioorganic & Medicinal Chemistry

journal homepage: www.elsevier.com/locate/bmc

A specific protein disorder catalyzer of HIV-1 Nef

Adrien Lugari [a], Sebastian Breuer [b], Thibault Coursindel [c], Sandrine Opi [d,e,f], Audrey Restouin [d,e,f], Xiaoli Shi [a,g], Alexis Nazabal [h], Bruce E. Torbett [b], Jean Martinez [c], Yves Collette [d,e,f], Isabelle Parrot [c], Stefan T. Arold [i,*], Xavier Morelli [a,*]

[a] IMR Laboratory, CNRS-UPR 3243, Centre National de la Recherche Scientifique, Institut de Microbiologie de la Méditerranée (IMM) and Aix-Marseille Universités, 31 Chemin Joseph Aiguier, 13402 Marseille Cedex 20, France
[b] Department of Molecular and Experimental Medicine, The Scripps Research Institute, 10550 North Torrey Pines Road, La Jolla, CA 92037, USA
[c] Institut des Biomolécules Max Mousseron (IBMM), UMR 5247 CNRS-Université Montpellier 1–Université Montpellier 2, CC17-03, Place Eugène Bataillon, 34095 Montpellier Cedex 5, France
[d] INSERM U891, Centre de Recherche en Cancérologie de Marseille, Marseille F-13009, France
[e] Institut Paoli-Calmettes, Marseille F-13009, France
[f] Université de la Méditerranée, Marseille F-13007, France
[g] State Key Laboratory of Structural Chemistry, Fujian Institute of Research on the Structure of Matter, Chinese Academy of Sciences, 155 Yang Qiao Xi Lu, Fuzhou, Fujian 350002, China
[h] CovalX AG, Grabenstrasse 11A, Schlieren CH-8952, Switzerland
[i] Department of Biochemistry and Molecular Biology, Unit 1000, The University of Texas MD Anderson Cancer Center, 1515 Holcombe Boulevard, Houston, TX 77030-4009, USA

ARTICLE INFO

Article history:
Received 31 August 2011
Revised 11 October 2011
Accepted 17 October 2011
Available online 20 October 2011

Keywords:
HIV-1 Nef inhibitor
Molecular modeling
Thermostability
Mass spectrometry
Protein–protein interaction inhibitor

ABSTRACT

The HIV-1 auxiliary protein Nef is required for the onset and progression of AIDS in HIV-1–infected persons. Here, we have deciphered the mode of action of a second-generation inhibitor of Nef, DLC27-14, presenting a competitive IC_{50} of ~16 μM measured by MALDI-TOF experiments. Thermal protein denaturation experiments revealed a negative effect on stability of Nef in the presence of a saturating concentration of the inhibitor. The destabilizing action of DLC27-14 was confirmed by a HIV protease-based experiment, in which the protease sensitivity of DLC27-14–bound Nef was three times as high as that of apo Nef. The only compatible docking modes of action for DLC27-14 suggest that DLC27-14 promotes an opening of two α-helices that would destabilize the Nef core domain. DLC27-14 thus acts as a specific protein disorder catalyzer that destabilizes the folded conformation of the protein. Our results open novel avenues toward the development of next-generation Nef inhibitors.

1. Introduction

During HIV-1 infection, HIV-1 auxiliary proteins such as Nef interact with many host proteins. These host–pathogen protein–protein interactions (PPIs) contribute crucially to the efficiency of viral infection, pathogenicity, and disease progression.[1–4] Numerous cellular partners of Nef have been identified, and they can be divided into two groups: proteins involved in the trafficking of cell surface receptors and proteins involved in cell signaling pathways.[5] Most of these PPIs involve binding to the Nef core domain (residues 56–206), a stable globular domain that contains a proline-rich motif, which allows the binding of Src homology 3 (SH3) kinase domains.[6] The biological properties of the Nef:SH3 domain complex, as well as the structural data available for this interaction[7,8], have led Nef to be considered as a suitable model for a structure-based drug design program.[6]

In this emerging field of PPI inhibition to target host–pathogen interactions, we identified in 2007 the first PPI inhibitor targeting the HIV-1 Nef:SH3 interaction.[9] This compound, DLC27 (Supplementary Fig. S1, panel a), was developed by coupling a virtual screening method to medium-throughput biological tests, the so-called 2P2I (protein–protein interaction inhibition) method. According to our previous analysis[9], DLC27 competes for the SH3 domain through specific binding to the region of Nef that binds to the SH3 RT loop (Supplementary Fig. S1, panel b). This RT loop binding region includes a mostly hydrophobic groove delimited by Nef residue Trp113.

In the present work, we used numerous biological and biophysical methods to test more than 30 DLC27 derivatives. Among these, we identify DLC27-14 as a promising and unusual

Abbreviations: HIV-1, human immunodeficiency virus-1; AIDS, acquired immune deficiency syndrome; PPIs, protein–protein interactions; SH3, Src homology 3; ITC, isothermal titration calorimetry; SPR, surface plasmon resonance; MALDI-TOF MS, matrix-assisted laser desorption/ionization-time-of-flight mass spectrometry; NMR, nuclear magnetic resonance; HSQC, heteronuclear single quantum coherence spectroscopy; STD, saturation transfer difference; DSLS, differential static light scattering.

* Corresponding authors. Tel.: +33 (0)491 164 501; fax: +33 (0)491 164 540 (X.M.); tel./fax: +1 713 792 6059 (S.T.A.).

E-mail addresses: starold@mdanderson.org (S.T. Arold), morelli@ifr88.cnrs-mrs.fr (X. Morelli).

0968-0896/$ - see front matter © 2011 Elsevier Ltd. All rights reserved.
doi:10.1016/j.bmc.2011.10.051

second-generation inhibitor of HIV-1 Nef, because DLC27-14 acts as a specific protein disorder catalyzer that destabilizes the folded conformation of the Nef core domain. Thus DLC27-14 could act as a potent antiviral compound.

2. Results and discussion

2.1. Discovery of potential lead compounds from DLC27 derivatives

DLC27 is a dual-head compound bearing a polar head with a carboxylic acid group and an apolar head composed of a *tert*-butyl in the *para* position of a phenyl cycle. The heads are separated by a carbamate-type linker (Supplementary Fig. S1, panel a). According to the binding model for DLC27 derived previously[9], the apolar head of the compound inserts itself into the hydrophobic RT loop binding region of the SH3 domain binding surface of Nef (Supplementary Fig. S1, panel b, region within gray dashed line). This hydrophobic groove is delimited by Nef residue Trp113 and accommodates residue 96 of the SH3 RT loop (according to the sequence of the Fyn SH3 domain)[7,8], which is critical for the Nef:SH3 interaction.[10] Indeed, Nef has a canonical polyproline SH3 recognition sequence, but additional contacts occur with the RT loops of the SH3 domains of the Src family kinases Hck and Fyn, in particular with SH3 residue 96 (using Fyn numbering). This tertiary recognition enhances significantly the specificity and affinity of these SH3 domains for HIV-1 Nef.[10–12] The Nef binding pocket for SH3 residue 96 is therefore a hot spot for the Nef:SH3 interaction and an attractive target for inhibitors.

We identified an additional hydrophobic pocket in the structure of the Nef:SH3 complex, adjacent to the binding pocket for residue 96. (Supplementary Fig. S1, panel b, region within red dashed line). We therefore decided to synthesize new DLC27 derivatives that could interact with this new pocket by an extension of the apolar head of DLC27. We expected this additional interaction to result in molecules that have higher affinity and specificity for Nef than DLC27.

We synthesized 30 DLC27 derivatives, named DLC27-1 to DLC27-30, by replacing the apolar head of DLC27 with various longer chemical groups with hydrophobic properties. All the compounds were tested in cell-based assays, as previously described by Betzi et al[9] Unfortunately, all the newly synthesized compounds had very low solubility (which is expected according to their calculated log*D* values), and thus no useful data could be obtained from these assays.

2.2. DLC27-14 is an improved inhibitor of the Nef:SH3-Hck complex

Because of the very low solubility, we could not obtain dissociation constants (K_d) for the compounds using classical biophysical methods such as isothermal titration calorimetry (ITC) or surface plasmon resonance (SPR). We therefore developed a mass-spectroscopy (MS)–based method to assess the capacity of the most promising DLC27 derivatives to inhibit the Nef:SH3-Hck complex. This technique, based on MALDI-TOF MS, enabled us to assess the potency of an inhibitor to block the formation of a protein complex in the presence of a bridging agent. This method successfully produced binding data, because it is relatively insensitive to DMSO (which is needed to solubilize the compounds) and to protein destabilization.

When applied to the Nef:SH3-Hck complex, we detected three major peaks, which were assigned to Nef and SH3-Hck in monomeric forms and to the Nef:SH3-Hck complex (Fig. 1, panel a). In the presence of DLC27, we observed a decrease in the peak corresponding to the Nef:SH3-Hck complex, which was associated with increases in the peaks corresponding to the monomeric forms of the proteins (Fig. 1, panel a). Adding DLC27 thus partially inhibits formation of the Nef:SH3-Hck complex. At the same concentration, one derivative compound, DLC27-14, totally inhibited formation of the Nef:SH3-Hck complex (Fig. 1, panel b). DLC27-14 therefore acts as a more potent inhibitor of Nef:SH3-Hck complex formation than does DLC27. To confirm these results, we performed several experiments at different compound concentrations and derived an IC_{50} of 16 μM for the inhibition of the Nef:SH3-Hck complex by DLC27-14 (Fig. 1, panel c). The amount of DLC27 needed to derive an IC_{50} value was significantly higher (not saturating at a concentration of 100 μM), indicative of an IC_{50} >50 μM.

DLC27-14 has a second phenyl cycle, which extends the apolar head of DLC27, as shown in Figure 2, panel a. The chemical pathway used to synthesize DLC27-14 is presented in Figure 2, panel b.

2.3. In silico modeling of DLC27 derivatives bound to Nef

To structurally characterize the binding mode of DLC27-14 on Nef, we set up nuclear magnetic resonance (NMR) experiments and crystallization assays. Those experiments, including NMR heteronuclear single quantum coherence spectroscopy (HSQC) and saturation transfer difference (STD) experiments as well as soaking and co-crystallization experiments, failed to yield exploitable data because the presence of the compound in DMSO induced Nef precipitation in solution or melting of Nef crystals even at less than equimolar ratios. We therefore used in silico docking methods to obtain structural insights into the Nef:DLC27-14 complex.

Figure 3, panel a shows the binding model of DLC27 on Nef, proposed by Betzi et al[9] Surprisingly, using the same docking program and protein files, we could not dock DLC27-14 onto the Nef surface. Effectively, in our DLC27 binding model the apolar head group of DLC27 pushes against a hydrophobic surface contributed by Trp113 and, to a lesser extent, Phe90. DLC27-14 is too long to fit into the RT-loop binding pocket as does DLC27. However DLC27-14 is also incapable of reaching over the barrier established by the side chain of Trp113 to attain the second adjacent hydrophobic pocket. Thus, to allow fitting DLC27-14 onto the Nef surface, the Trp113 side chain has to move away. This is plausible because Trp113 has an above-average mobility in the crystal structure of the apo-Nef core domain (mean Trp113 B-factor = 76.8 Å^2 compared with an overall B-factor = 37.5 Å^2 for all atoms of the structure).[7] From the structure, there are two ways for the Trp113 side chain to move away: (i) by rotating towards the second hydrophobic pocket. This movement is plausible because it corresponds to only a subtle exaggeration of the movement that the Trp113 side chain undergoes to accommodate the bulky Fyn Arg96 residues.[7] (ii) By using a different rotamer, which rotates the Trp113 side chain out of the pocket. A suitable rotamer corresponds to the second most probable conformation of the residue in solution, according to the SYBYL tools (Tripos). Both plausible Trp113 side chain conformations create enough space to allow docking of DLC27-14. In both cases the apolar extension of DLC27-14 reaches into the adjacent second hydrophobic pocket of Nef while the polar head of the compound stills occupies the SH3 RT loop binding site. In doing so, DLC27-14 disrupts a hydrophobic connection between the side chains of Trp113 and Phe90. We therefore hypothesized that DLC27-14 (as well as DLC27, to some extent) catalyzes Nef unfolding by destabilizing a large hydrophobic contact of its core domain.

2.4. Characterization of DLC27 and DLC27-14 mode of Inhibition

To decipher the mode of action of the compounds, we used a differential static light scattering (DSLS) based thermal protein denaturation assay on Nef in complex with DLC27 and DLC27-14 molecules. Interestingly, DLC27 in DMSO strongly decreased the

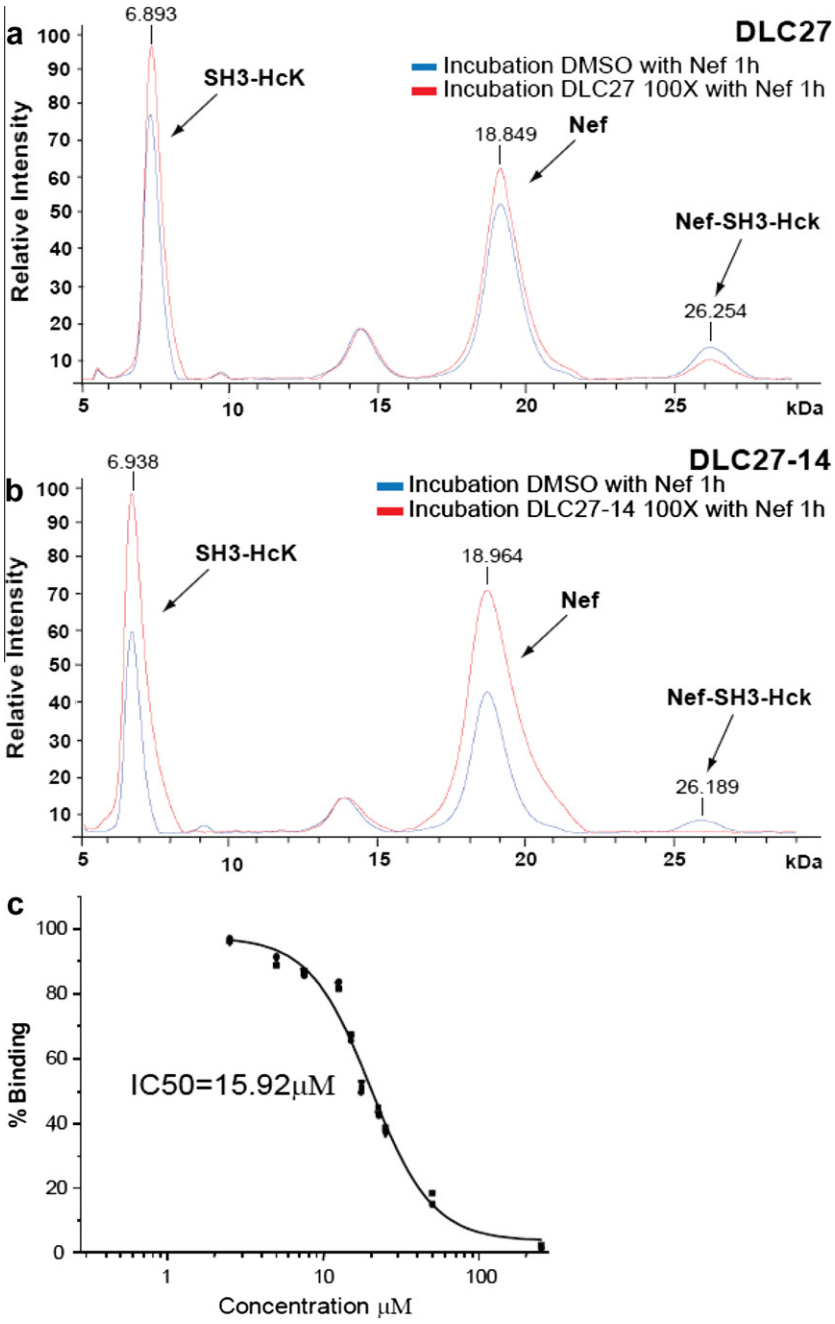

Figure 1. Inhibition of the Nef:SH3-Hck complex, assessed by high-mass MALDI-TOF. (a) High-mass MALDI-TOF spectrum of the Nef:SH3-Hck protein complex before (blue) and after (red) 1 h of incubation with DLC27 100×. The complex was detected with MH^+ = 26.254 kDa. The two subunits forming the complex were also detected, with MH^+ = 6.891 kDa and MH^+ = 18.849 kDa (b) High-mass MALDI-TOF spectrum of the Nef:SH3-Hck protein complex before (blue) and after (red) 1 h of incubation with DLC27-14 100×. The complex was detected with MH^+ = 26.189 kDa. The two subunits forming the complex were also detected, with MH^+ = 6.938 kDa and MH^+ = 18.964 kDa. (c) Effect of DLC27-14 concentration on the percentage of binding for the Nef:SH3-Hck protein complex. The percentage of protein complex binding obtained by high-mass MALDI-TOF experiments was plotted as a function of inhibitor concentration (logarithmic scale) to determine the IC_{50} value of DLC27-14.

aggregation temperature of Nef by ~10° compared with a control with Nef and DMSO only (Fig. 4, panel a). DLC27 thus already destabilizes Nef. As DLC27-14 had very low solubility and a propensity to precipitate Nef in solution, we could not obtain DSLS data for this compound even at very low temperatures. Because of its similarity to DLC27 and our binding and modeling data, we expected that the DLC27-14 also destabilizes Nef.

2.5. Proteolytic sensitivity to HIV protease

A significant destabilization of the Nef core domain is expected to increase the sensitivity of Nef to proteolysis. We therefore compared how HIV-1 protease cleaves Nef at the Trp57/Leu58 HIV protease cleavage site in presence or absence of DLC27 and DLC27-14 using a cleavage enzyme-cytometric bead array (CE-CBA) experiment (Fig. 4b and c and Supplementary Fig. S2). This substrate cleavage assay relies on native Nef protein expressed as a fluorescent reporter fusion protein (GST-Nef-mVenus) coupled to anti-GST antibody coated beads. Nef cleavage by the HIV protease is then followed through the loss of fluorescence on the beads utilizing flow cytometry.[13] The CE-CBA allows precise determination of alterations in protease catalytic efficiency and facilitates the identification of small molecule inhibitors of the protease or its substrate Nef. Structural analysis shows that the Trp57/Leu58

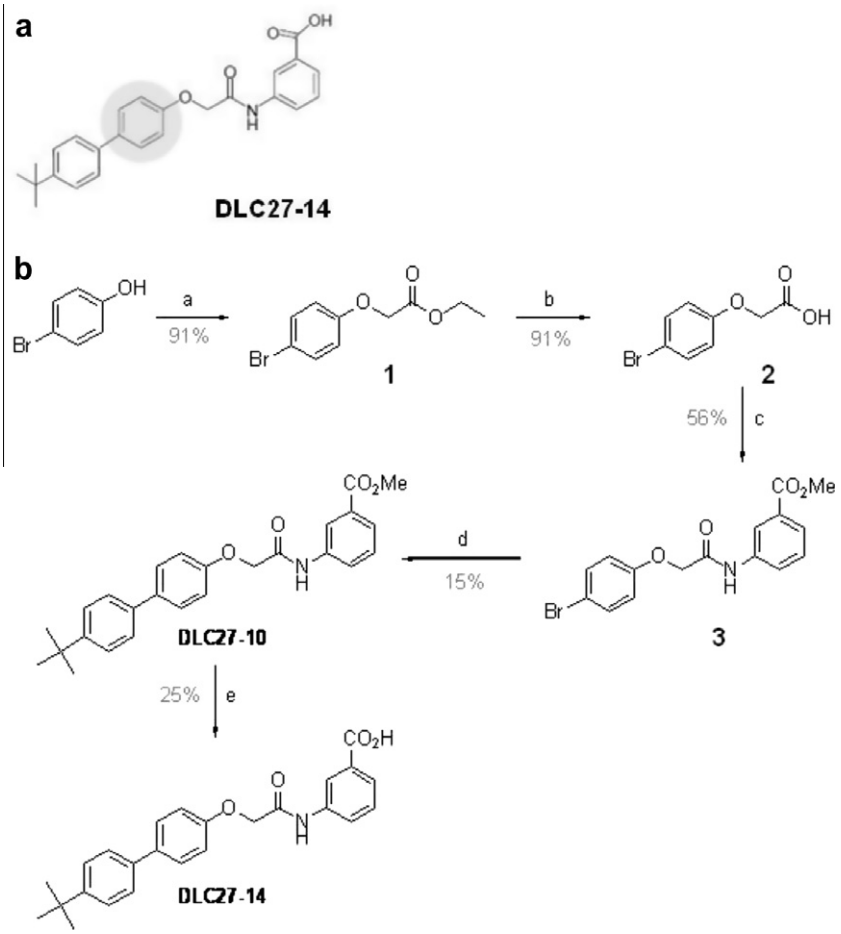

Figure 2. DLC27-14 structure and synthesis. (a) Structure of DLC27-14. The gray circle represents the additional phenyl cycle compared with DLC27. (b) Chemical synthesis pathway of the most potent derivatives of DLC27.

cleavage site interacts with the second hydrophobic pocket in the Nef core domain in proximity of Trp113.[14,15] We therefore reasoned that destabilization of the Nef core by Trp113 conformational changes exposes the HIV protease cleavage site. Indeed, DLC27 accelerated Nef proteolysis, with EC_{50} = 109.1 ± 1.9 μM. DLC27-14 demonstrated an improved capacity to catalyze Nef proteolysis, with EC_{50} = 34.3 ± 3.7 μM. These results agree with those from our MS experiments and validate that our optimized compound acts as a specific protein disorder catalyzer that destabilizes the folded conformation of the Nef core domain and thus increases its sensitivity to HIV protease. The destabilizing properties of these compounds would explain why we could not obtain structural data on their binding mode using NMR or X-ray crystallography.

3. Summary and conclusions

In the present work, we evaluated 30 chemically synthesized DLC27 derivatives as potential second-generation inhibitors of the Nef:SH3-Hck complex. In these compounds, the apolar head of DLC27 was replaced with various longer chemical groups with hydrophobic properties. As we could not evaluate the binding capacity of these new-generation inhibitors using standard biophysical experiments such as NMR, ITC, SPR, or X-ray crystallography, we developed an original in vitro experiment using MALDI-TOF MS that enabled us to evaluate IC_{50} values. We found the compound DLC27-14 to be a more potent and more efficient inhibitor than DLC27 of the Nef:SH3-Hck domain interaction, with an IC_{50} of about 16 μM. DSLS experiments and analysis of cleavage of Nef by the HIV protease showed that DLC27 and DLC27-14 decreased the Nef stability and enhanced proteolytic sensitivity. In silico molecular modeling suggested that DLC27-14 (and to a lesser extend DLC27) destabilizes the Nef core domain by disrupting a hydrophobic barrier established by Trp113. Because of this solubility issue, we did not succeed to measure a biological activity for our DLC27-X series, except for slight cell toxicity. Indeed, up to 40 μM DLC27 only reduced cell viability to 86.6%, while 40 μM of DLC27-14 reduced cell viability down 73% (Supplementary Fig. S3). Thus, a major issue towards further development of this DLC27 series will be to increase the solubility of the compounds, without further impacting on cell viability, but displaying anti-viral activity by targeting the function of Nef on virion infectivity and anti-viral defense (CD4 and MHC I down regulation). Thus we demonstrated that the new optimized compound, DLC27-14, acts as a specific protein disorder catalyzer and thus could act as a potent antiviral compound.

4. Methods

4.1. Synthesis of Compounds

All solvents were dried and freshly distilled before use. All reactions were carried out under an atmosphere of dry argon in flame-dried glassware. Reactions were magnetically stirred and monitored by thin-layer chromatography using silica gel plates (Kieselgel 60 F254, Merck) or by analytical HPLC. For validation, we carried out NMR experiments on the compounds. For details of HPLC and NMR experiments, please refer to Supplementary data.

For details about the synthesis of (4-bromo-phenoxy)-acetic acid ethyl ester,[16] (4-bromo-phenoxy)-acetic acid,[17] 3-[2-(4-bromo

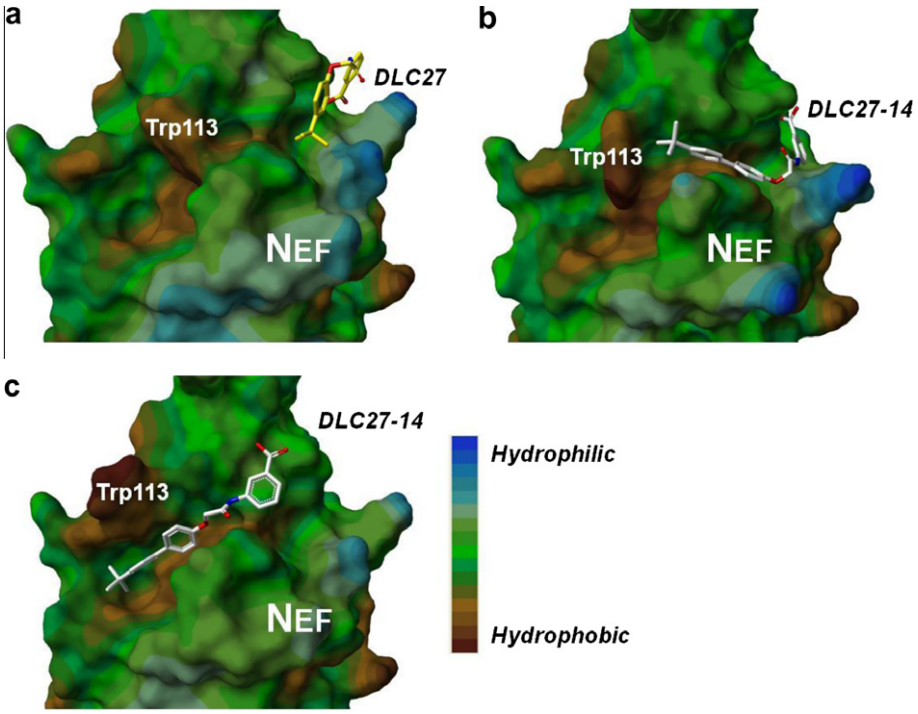

Figure 3. DLC27 and DLC27-14 binding models on Nef. (a) Docking model of DLC27 on surface representation of Nef, colored according to lipophilic potential (PDB code: 1AVZ, chain B). The docking model was obtained using Surflex-Dock (version 2.4) (Tripos) and represented using LITHIUM software (Tripos). (b and c) Docking models of DLC27-14 on Nef. The Nef protein presents an alternative conformation for the residue Trp113, as explained in Methods. For (b), the hydrophobic pocket was built based on PDB code 1AVZ (chain B) and Trp113 was rotated by about 35° towards the second pocket using the 'regularize zone' mode in COOT.[21] For (c), the alternative Trp113 conformation corresponds to the second most populated conformation for residue Trp113 according to Sybyl 'set sidechain conformation' tool.

-phenoxy)-acetylamino]-benzoic acid methyl ester,[18] 3-[2-(4′-*tert*-butyl-biphenyl-4-yloxy)-acetylamino]-benzoic acid methyl ester (DLC27-10), and 3-[2-(4′-*tert*-butyl-biphenyl-4-yloxy)-acetylamino]-benzoic acid (DLC27-14), please refer to Supplementary data.

4.2. Protein expression and purification

The HIV-1 Nef core domain (residues 56–206) and the Hck SH3 domain were expressed in *E. coli* BL21 DE3 as GST (glutathione *S*-transferase) fusion proteins. The purification used was derived from that described in Franken et al.[19] Cells were grown at 37 °C until OD_{600} = 0.6 was reached and then induced using 0.2 mM IPTG and cultured overnight at 20 °C. Cells were pelleted by centrifugation (15 min at 8,000*g*), and pellets were resuspended in 20 mM Tris (pH 8.0), 150 mM NaCl, 2 mM EDTA, and 5 mM dithiothreitol (DTT). After French press and centrifugation (45 min at 45000*g*), the supernatant was purified by GST-affinity column chromatography (GE Healthcare Life Sciences). After incubation of peak fractions with thrombin protease (20:1) at 4 °C, the cleaved GST tag was removed with a second GST-affinity column. Protein peak fractions were then loaded onto a Superdex 75 column and eluted with 50 mM PO_4 (pH 7.0), 150 mM NaCl, 5 mM DTT, and 2.5 mM EDTA for Nef and 20 mM HEPES (pH 8.0), 150 mM NaCl, and 2 mM EDTA for SH3-Hck. Purified proteins were further concentrated and stored at −80 °C.

4.3. MS experiments

All the high-mass measurements were performed using a MALDI mass spectrometer (ABI 4800 MALDI-TOF/TOF, ABSCIEX) equipped with the HM2 high-mass detection system (CovalX). The CovalX HM2 system is designed to optimize ion detection in the high-mass range, up to 1500 kDa, with nanomolar sensitivity. Previously purified Nef (5 μM, 4.5 μL) was mixed with 0.5 μL of DLC27 or DLC27-14, diluted in 100% DMSO with a concentration of 50 μM (1×), 100 μM (2×), 150 μM (3×), 250 μM (5×), 300 μM (6×), 350 μM (7×), 450 μM (9×), 500 μM (10×), or 5 mM (100×). The mixture was incubated for 1 h at rt. After incubation of Nef with each inhibitor, the mixture was mixed with 5 μL of SH3-Hck (5 μM). The mixture was then incubated for 1 h at rt. The final concentrations of the proteins in the mixture were 2.5 μM for Nef and 2.5 μM for SH3-Hck. After incubation, the samples were submitted to cross-linking using the K100 MALDI MS stabilization kit (CovalX). First, 1 μL of the cross-linking reagent (2 mg mL^{-1}) was added to each solution, and the mixture was incubated for 1 h. After incubation, 1 μL of each mixture obtained was mixed with 1 μL of recrystallized sinapinic acid matrix (10 mg $^{-1}$) in acetonitrile/water (1:1, v/v), trifluoroacetyl 0.1%. After mixing, 1 μL of each sample was spotted onto the MALDI plate. The analysis was performed in triplicate. After crystallization at rt, the plate was introduced into the MALDI mass spectrometer and analyzed immediately. See Supplementary data for details of the analysis.

4.4. Computer files and docking experiments

Both DLC27 and DLC27-14 were designed as standard .mol2 files using the SYBYL chemical structure drawing tool (Tripos) and further minimized. For docking experiments, the Nef structure was taken from the crystallographic structure of the Nef protein in complex with the Fyn SH3 domain (PDB code: 1AVZ, chain B)[7] as described by Betzi et al[9] All dockings were computed using the Surflex-Dock (version 2.4) Geom X algorithm within the SYBYL suite (Tripos). Please refer to Supplementary data for details.

4.5. DSLS-based thermal protein denaturation

Thermal protein denaturation based on DSLS was performed using a multiwell instrument (StarGazer-384, Harbinger Biotech),

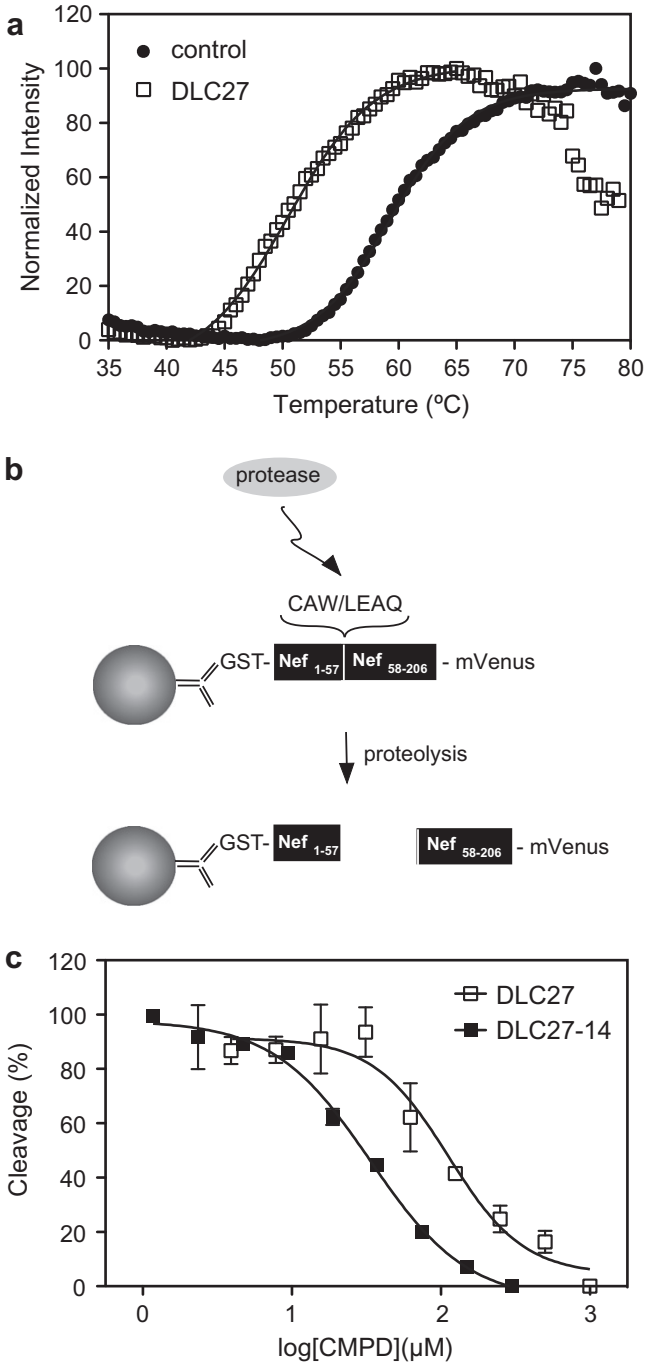

Figure 4. Biochemical profiling of DLC27 and DLC27-14. (a) Thermostability of Nef in complex with DLC27. Shown is a representative thermal protein denaturation experiment (DSLS-based thermal protein denaturation curve of Nef in the presence of 200 μM compound). T_{agg} was calculated as mean ± SEM of three independent experiments. T_{agg} (Nef + DLC27) = 50.29 ± 0.03 °C, and T_{agg} (Nef + DMSO) = 58.83 ± 0.25 °C. (b) Schematic description of the cleavage enzyme–cytometric bead array (CE-CBA). A recombinant reporter fusion protein (GST-Nef-mVenus) was immobilized on cytometric beads labeled with anti-GST antibody. The HIV protease recognizes and cleaves at the specific cleavage site of Nef, liberating Nef's core domain and mVenus reporter protein. Loss of mVenus decreases the fluorescence signal on the beads, which can be quantified by flow cytometry. (c) Effects of the compounds on Nef sensitivity to proteolysis. The effect of the compounds on the stability of the Nef structure was analyzed by observing the proteolytic processing of Nef by HIV protease. Shown is the percentage of cleavage as a function of compound concentration (normalized to the bead fluorescence of the DMSO control as 0% cleavage and the intrinsic bead fluorescence as 100% cleavage). The relative EC_{50} value was calculated as described in Methods and presented as mean ± SEM of three independent experiments. For DLC27, EC_{50} = 109.1 ± 1.9 μM; for DLC27-14, EC_{50} = 34.3 ± 3.7 μM.

and His-tagged Nef protein was produced according to the procedure described in Breuer et al. 2006.[20] The aggregation temperature (T_{agg}) was determined by increasing the temperature of 10 μM His-tagged Nef from 25 °C to 85 °C in the presence of 10–200 μM compound in 50 mM HEPES (pH 7.5), 750 mM NaCl, and 1% (v/v) DMSO. T_{agg} was calculated by fitting a Boltzmann sigmoidal curve function using GraphPad Software version 5.0.

4.6. Enzymatic proteolysis

Nef cleavage mediated by HIV protease was measured using cleavage enzyme-cytometric bead array (CE-CBA) technology as described in Breuer et al. 2011.[13] Please refer to Supplementary data for details.

Acknowledgment

The project was supported by the ANRS (Agence Nationale de Recherche sur le SIDA et les Hépatites Virales) and the CNRS (Centre National de la Recherche Scientifique). This research is supported in part by the National Institutes of Health through MD Anderson's Cancer Center Support Grant (CA016672). A.L. and S.O. were supported by a fellowship from the ANRS. T.C. was supported by a fellowship from the MESR (Ministère de l'Enseignement Superieur et de la Recherche). X.S. was supported by a fellowship from the French Embassy in China. S.B. was supported by CHRP-F09-SRI-205. We are grateful to Dr. I. Engels and S. Espinola for providing valuable technical expertise with the DSLS-based thermal protein denaturation at the Genomics Institute of the Novartis Research Foundation. We also would like to greatly thank K. Muller for editorial assistance.

Supplementary data

Supplementary data associated with this article can be found, in the online version, at doi:10.1016/j.bmc.2011.10.051.

References

1. Peterlin, B. M.; Trono, D. *Nat. Rev. Immunol.* **2003**, *3*, 97.
2. Fackler, O. T.; Alcover, A.; Schwartz, O. *Nat. Rev. Immunol.* **2007**, *7*, 310.
3. Das, S. R.; Jameel, S. *Indian. J. Med. Res.* **2005**, *121*, 315.
4. Stevenson, M. *Nat. Med.* **2003**, *9*, 853.
5. Arold, S. T.; Baur, A. S. *Trends Biochem. Sci.* **2001**, *26*, 356.
6. Saksela, K. *Curr. Drug Targets Immune Endocr. Metabol. Disord.* **2004**, *4*, 315.
7. Arold, S.; Franken, P.; Strub, M. P.; Hoh, F.; Benichou, S.; Benarous, R.; Dumas, C. *Structure* **1997**, *5*, 1361.
8. Lee, C. H.; Saksela, K.; Mirza, U. A.; Chait, B. T.; Kuriyan, J. *Cell* **1996**, *85*, 931.
9. Betzi, S.; Restouin, A.; Opi, S.; Arold, S. T.; Parrot, I.; Guerlesquin, F.; Morelli, X.; Collette, Y. *Proc. Natl. Acad. Sci. U.S.A.* **2007**, *104*, 19256.
10. Lee, C. H.; Leung, B.; Lemmon, M. A.; Zheng, J.; Cowburn, D.; Kuriyan, J.; Saksela, K. *EMBO J* **1995**, *14*, 5006.
11. Moarefi, I.; LaFevre-Bernt, M.; Sicheri, F.; Huse, M.; Lee, C.; Kuriyan, J.; Miller, W. *Nature* **1997**, *385*, 650.
12. Collette, Y.; Arold, S.; Picard, C.; Janvier, K.; Benichou, S.; Benarous, R.; Olive, D.; Dumas, C. *J. Biol. Chem.* **2000**, *275*, 4171.
13. Breuer, S.; Sepulveda, H.; Chen, Y.; Trotter, J.; Torbett, B. E. *Biochemistry* **2011**, *50*, 4371.
14. Grzesiek, S.; Bax, A.; Hu, J. S.; Kaufman, J.; Palmer, I.; Stahl, S. J.; Tjandra, N.; Wingfield, P. T. *Protein Sci.* **1997**, *6*, 1248.
15. Breuer, S.; Schievink, S. I.; Schulte, A.; Blankenfeldt, W.; Fackler, O. T.; Geyer, M. *PLoS One* **2011**, *6*, e20033.
16. Sathisha, K. R.; Khanum, S. A.; Chandra, J. N.; Ayisha, F.; Balaji, S.; Marathe, G. K.; Gopal, S.; Rangappa, K. S. *Bioorg. Med. Chem.* **2011**, *19*, 211.
17. Khanum, S. A.; Khanum, N. F.; Shashikanth, M. *Bioorg. Med. Chem. Lett.* **2008**, *18*, 4597.
18. Lee, K.; Lee, J. H.; Boovanahalli, S. K.; Jin, Y.; Lee, M.; Jin, X.; Kim, J. H.; Hong, Y. S.; Lee, J. J. *J. Med. Chem.* **2007**, *50*, 1675.
19. Franken, P.; Arold, S.; Padilla, A.; Bodeus, M.; Hoh, F.; Strub, M. P.; Boyer, M.; Jullien, M.; Benarous, R.; Dumas, C. *Protein Sci.* **1997**, *6*, 2681.
20. Breuer, S.; Gerlach, H.; Kolaric, B.; Urbanke, C.; Opitz, N.; Geyer, M. *Biochemistry* **2006**, *45*, 2339.
21. Emsley, P.; Cowtan, K. *Acta Crystallogr., Sect. D Biol. Crystallogr.* **2004**, *60*, 2126.